Journal of Hazardous Materials 209–210 (2012) 99–110

Contents lists available at SciVerse ScienceDirect

Journal of Hazardous Materials

journal homepage: www.elsevier.com/locate/jhazmat

Equilibrium and kinetics study on hexavalent chromium adsorption onto diethylene triamine grafted glycidyl methacrylate based copolymers

Danijela D. Maksin[a], Aleksandra B. Nastasović[b,*], Aleksandra D. Milutinović-Nikolić[b], Ljiljana T. Suručić[c], Zvjezdana P. Sandić[d], Radmila V. Hercigonja[e], Antonije E. Onjia[a]

[a] University of Belgrade, Vinča Institute of Nuclear Sciences, P.O. Box 522, Belgrade, Serbia
[b] University of Belgrade, Institute of Chemistry, Technology and Metallurgy, Njegoševa 12, Belgrade, Serbia
[c] University of Belgrade, Faculty of Forestry, Kneza Višeslava 1, Belgrade, Serbia
[d] Faculty of Science, Mladena Stojanovića 2, Banja Luka, Bosnia and Herzegovina
[e] University of Belgrade, Faculty of Physical Chemistry, Studentski trg 12-16, 11001 Belgrade, Serbia

ARTICLE INFO

Article history:
Received 31 August 2011
Received in revised form
14 December 2011
Accepted 28 December 2011
Available online 10 January 2012

Keywords:
Chromium(VI) sorption
Glycidyl methacrylate
Diethylene triamine
Sorption kinetics
Equilibrium isotherms

ABSTRACT

Two porous and one non-porous crosslinked poly(glycidyl methacrylate-*co*-ethylene glycol dimethacrylate) [abbreviated PGME] were prepared by suspension copolymerization and functionalized with diethylene triamine [abbreviated PGME-deta]. Samples were characterized by elemental analysis, mercury porosimetry, scanning electron microscopy with energy-dispersive X-ray spectroscopy, and transmission electron microscopy. Kinetics of Cr(VI) sorption by PGME-deta were investigated in batch static experiments, in the temperature range 25–70 °C. Sorption was rapid, with the uptake capacity higher than 80% after 30 min. Sorption behavior and rate-controlling mechanisms were analyzed using five kinetic models (pseudo-first order, pseudo-second order, Elovich, intraparticle diffusion and Bangham model). Kinetic studies showed that Cr(VI) adsorption adhered to the pseudo-second-order model, with definite influence of pore diffusion. Equilibrium data was tested with Langmuir, Freundlich and Tempkin adsorption isotherm models. Langmuir model was the most suitable indicating homogeneous distribution of active sites on PGME-deta and monolayer sorption. The maximum adsorption capacity from the Langmuir model, Q_{max}, at pH 1.8 and 25 °C was 143 mg g^{-1} for PGME2-deta (sample with the highest amino group concentration) while at 70 °C Q_{max} reached the high value of 198 mg g^{-1}. Thermodynamic parameters revealed spontaneous and endothermic nature of Cr(VI) adsorption onto PGME-deta.

© 2012 Elsevier B.V. All rights reserved.

1. Introduction

The persistence of extremely toxic nondegradable heavy metals in the ecosystem presents serious environmental hazard, since these pollutants accumulate in living tissues throughout the food chain causing serious health problems [1]. Chromium, which is on the top-priority list of toxic pollutants defined by the U.S. Environmental Protection Agency (EPA), has a wide range of possible oxidation states [2]. However, chromium exists in the majority of terrestrial surface and aqueous environments primarily in two valence states, trivalent [Cr(III)] and hexavalent chromium [Cr(VI)] [3–5]. Cr(III) is less toxic than Cr(VI), but water-soluble Cr(III) species do not occur naturally and are unstable in the environment. Trivalent chromium is easily oxidized over a range of oxic conditions in aqueous media and solids [6]. Major sources of chromium contamination are electroplating, corrosion control, leather tanning industries, paints and pigments industry, photography, fungicide industry and ceramics or glass manufacturing [7,8]. The hexavalent form, reported to be five hundred times more toxic than the trivalent one [9], is classified as a known human carcinogen that modifies the DNA transcription process causing important chromosomal aberrations [10,11]. Also, it can cause kidney and gastric damage and epidermal irritation. The structural similarity of Cr(VI) anions to biologically important inorganic anions, such as SO_4^{2-} and PO_4^{3-}, is likely accountable for their ability to readily transverse cell membranes, via the sulfate transport system [1]. Cr(VI) anions incorporated into cells can oxidize biological molecules [12]. Because of the detrimental effect on human health, the maximum permissible levels of Cr(VI) in

* Corresponding author at: University of Belgrade – Institute of Chemistry, Technology and Metallurgy, Belgrade, Serbia. Tel.: +381 11 2635 839; fax: +381 11 2636 061.
E-mail addresses: dmaksin@vinca.rs (D.D. Maksin), anastaso@chem.bg.ac.rs, anastasovic@yahoo.com (A.B. Nastasović), snikolic@nanosys.ihtm.bg.ac.rs (A.D. Milutinović-Nikolić), ljilja_m@yahoo.com (L.T. Suručić), zvjezdana.sandic@gmail.com (Z.P. Sandić), radah@ffh.bg.ac.rs (R.V. Hercigonja), onjia@vinca.rs (A.E. Onjia).

0304-3894/$ – see front matter © 2012 Elsevier B.V. All rights reserved.
doi:10.1016/j.jhazmat.2011.12.079

Nomenclature

a_e	initial adsorption rate from Elovich model (mmol g^{-1} min^{-1})
α	constant calculated from slope of linear Bangham's plots
b_e	Elovich's parameter related to extent of surface coverage and activation energy for chemisorption (g $mmol^{-1}$)
B_T	constant related to the heat of adsorption from Tempkin isotherm model
C	concentration of Cr(VI) in aqueous phase at time τ (mg g^{-1})
C_i	initial Cr(VI) concentration (mmol L^{-1})
C_e	Cr(VI) concentration in aqueous phase at equilibrium (mmol L^{-1})
C_{id}	intercept of intraparticle diffusion plot (mmol g^{-1})
C_s	dosage of adsorbent (g L^{-1})
C_t	Cr(VI) concentration (mmol L^{-1}) in aqueous phase after time τ
ΔG	Gibbs free energy change (kJ mol^{-1})
ΔH	enthalpy change (kJ mol^{-1})
ΔS	entropy change (kJ mol^{-1} K^{-1})
E_a	activation energy (kJ mol^{-1})
F_e	fraction adsorbed at equilibrium
m	amount of sorbent used for sorption experiment (g)
h	initial adsorption rate from pseudo-second-order model (mmol g^{-1} min^{-1})
k_b	constant calculated from intercept of linear Bangham's plots (g^{-1})
K_F	Freundlich isotherm constant $((mg\,g^{-1})/(mg\,L^{-1})^{1/n})$
k_1	pseudo-first-order rate constant (min^{-1})
k_2	pseudo-second order rate constant (g^{-1} $mmol^{-1}$ min^{-1})
k_{id}	intraparticle diffusion rate constant (mmol g^{-1} $min^{-0.5}$)
K_L	Langmuir isotherm constant (L mg^{-1})
K_T	Tempkin isotherm constant (L mg^{-1})
n	Freundlich isotherm exponent
Q	amount of sorbed metal ions at time τ (mmol g^{-1})
Q_e	amount of sorbed metal ions at equilibrium (mmol g^{-1} or mg g^{-1})
Q_{max}	monolayer capacity of the adsorbent (mg g^{-1})
R	universal gas constant (8.314 J mol^{-1} K^{-1}).
R^2	coefficient of determination
τ	time (min)
t	temperature (°C)
T	absolute temperature (K)
V	solution volume (L)

drinking water and wastewater were set by EPA at 20 and 200 μg L^{-1}, respectively [4]. Since the health effects are determined largely by the oxidation state, different guideline values for chromium(III) and chromium(VI) should be derived. However, current analytical methods and variable speciation of chromium in water favor a guideline value for total chromium which is set at 0.05 mg L^{-1} at this time, according to the World Health Organization [8].

Different techniques, like adsorption [1,13], precipitation following reduction [14], reverse osmosis [15], electrolytic recovery techniques [16], ion exchange [17] and liquid–liquid extraction [18] are used for chromium removal from industrial effluents. Among them, adsorption is one of the most popular methods for the removal of chromium from wastewaters [1]. A number of different types of adsorbents, like lignocellulosic materials [10], activated carbon [11], chitin and chitosan [13,19–21], various biomass materials [22–27], natural and artificial minerals [28,29], starch [30] and synthetic polymer adsorbents [1,5,17,31–37] were proven to remove chromium from aqueous solutions.

Polymers have some significant advantages over other adsorbent materials; for example, polymers can be readily manufactured in a wide range of physicochemical properties (size, size distribution, porosity, hydrophobicity, etc.) and they are modifiable by inserting various ligands into the structure in order to produce specific sorbents [5]. Macroporous crosslinked glycidyl methacrylate (GMA) copolymers, produced by radical suspension copolymerization, in the shape of regular beads of required size and porosity, were already successfully used for heavy and precious metals sorption [38–42], as well as dye adsorbents [43–45].

In our previous research, non-competitive and Cr(VI) competitive experiments with Cu(II), Co(II), Cd(II) and Ni(II) ions showed fast kinetics and high Cr(VI) uptake capacities at acidic pH [46]. This study was aimed to explore the relations between the PGME functionalization and porosity, and the mechanism of Cr(VI) anions uptake onto the amino-functionalized PGME surface.

In this paper, two porous samples of macroporous GMA and ethylene glycol dimethacrylate (EGDMA) copolymer [PGME] with different porosity parameters were synthesized by suspension copolymerization, as well as one non-porous sample, and functionalized with diethylene triamine. The amino-functionalized copolymers were evaluated as chromium(VI) adsorbents, in a batch static system, under non-competitive conditions. To identify the nature of adsorption kinetics and evaluate the kinetic constants, as well as to establish the rate limiting step of hexavalent chromium adsorption and postulate the mechanism of Cr(VI) removal by PGME-deta copolymers, kinetic data at four different temperatures were analyzed using five kinetic models (pseudo-first, pseudo-second order, Elovich equation, intraparticle diffusion and Bangham model). The linearized Langmuir, Freundlich and Tempkin equations were used to fit the equilibrium isotherms for these chromium-sorbent systems. The thermodynamic parameters were also evaluated from the adsorption measurements.

2. Experimental

2.1. Materials and methods

All chemicals were analytical grade products and used as received. Chromium(VI) solutions were prepared from reagent grade $K_2Cr_2O_7$ (Sigma–Aldrich), using deionized water (Milli-Q Millipore, 18 MΩ cm^{-1} conductivity).

Pore size distributions were determined by a high pressure mercury intrusion porosimeter Carlo Erba Porosimeter 2000, operating in the interval of 0.1–200 MPa. Sample preparation was performed at room temperature and pressure of 0.5 kPa. The specific surface areas (S_{BET}) of non-porous samples PGME3 and PGME3-deta were determined by the BET method from the low-temperature nitrogen adsorption isotherms obtained by Sorptomatic 1990 Thermo Finnigan at −196 °C. Samples were outgassed at 50 °C and 1 mPa for 6 h.

Concentrations of Cr(VI) were determined by flame atomic absorption spectroscopy (FAAS) (PerkinElmer 3100). Standard statistical methods were used to determine the mean values and standard deviations for each set of data. Each experiment was repeated three times or more if necessary. Relative standard deviations did not exceed 5.0%. Additionally, possible presence of Cr(III) was tested colorimetrically. Concentration of Cr(VI) was measured by 1,5-diphenylcarbazide colorimetric method at 540 nm wavelength using UV Spectrophotometer (Thermo Electron Nicolet

Evolution 500) [48]. It was found that the results obtained using this method were the same as the data obtained by FAAS under the same conditions (within the calculated relative standard deviation for FAAS of 5.0%). Therefore, FAAS was proven to be an applicable method for this study. Surface and interior morphology of PGME beads was investigated by a scanning electron microscope at desired magnifications (SEM) (JEOL, JSM-6460 LV, Tokyo, Japan), after coating with a thin layer of gold under reduced pressure. Cr(VI) loaded particles were examined using energy dispersive spectroscopy (EDS) analyzer (Oxford Instruments X-Max 20 mm^2).

Transmission electron microscopy (TEM) analysis was performed on a JEOL-1200EX transmission electron microscope operating at an accelerating voltage of 100 kV. Loaded copolymer particles were embedded in an epoxy resin (Epofix, Electron Microscopy Sciences) and cured overnight at 40 °C. Samples were subsequently microtomed to a thickness of about 80 nm using a Leica Ultracut UCT-ultramicrotome and a Diatome diamond knife at room temperature. The microtomed sections were floated on water and subsequently placed on copper grids. Multiple images of samples were recorded.

2.2. Preparation of PGME-deta samples

Two macroporous copolymer samples were prepared by a radical suspension copolymerization and purified after the completion of reaction, as described elsewhere (content of crosslinking monomer, EGDMA, in two porous copolymer samples, PGME1 and PGME2, was 40 and 20 mass%, respectively) [47]. Non-porous sample PGME3 was synthesized without inert component; the monomer phase consisting of 39.0 g GMA and 26.0 g EGDMA and containing 0.65 g of 2,2′-azobisiso-butyronitrile (AIBN), was suspended in the aqueous phase containing 200.0 g of deionized water and 2.00 g of poly(N-vinyl pyrrolidone). The temperature program, the duration and the stirring conditions were the same as for the macroporous samples [47]. The resulting crosslinked beads were sieved and the fraction with average particle diameter (D) in the range 150–300 μm was used in subsequent reactions.

All synthesized PGME samples were functionalized with diethylene triamine using the procedure described elsewhere [47]. The modified samples were labeled as PGME1-deta, PGME2-deta and PGME3-deta (additional label-deta designates functionalization with diethylene triamine).

2.3. Chromium sorption batch experiments

The sorption kinetics of Cr(VI) ions from acidic aqueous solutions (C_i = 0.01, 0.02, 0.05 and 0.1 M; pH = 1.8) was investigated in batch experiments under non-competitive conditions, at room temperature (t = 25 °C). Additional experiments were performed at pH 1.8, C_i = 0.1 M, at 40, 55 and 70 °C to assess the effect of temperature.

For determination of Cr(VI) sorption rates, 0.50 g of copolymer was contacted with 50 mL of metal salt solution. In each experiment, 0.5 mL aliquots were removed at appropriate times (1, 5, 15, 30, 60, 90 and 180 min), diluted to 50 mL and analyzed by FAAS.

The amount of metal ions adsorbed onto unit mass of copolymer beads (sorption capacity, mmol g^{-1}) was calculated using the following equation:

$$Q = \frac{(C_i - C) \cdot V}{m} \quad (1)$$

Complete adsorption isotherms were obtained in static experiments by placing rations of 0.50 g of copolymer in contact with a series of Cr(VI) solutions in the concentration range 0.01–0.1 M, at room temperature and pH = 1.8. Equilibrium time was 3 h.

Table 1
Porosity parameters of the initial and functionalized PGME samples [47].

Sample	S_{Hg}, $m^2\ g^{-1}$	V_S, $cm^3\ g^{-1}$	$d_{V/2}$, nm
PGME1	59	0.96	74
PGME2	40	0.96	148
PGME1-deta	55	0.91	96
PGME2-deta	29	0.89	184

Preliminary investigations of Cr(VI) uptake dynamics at unadjusted pH were conducted from the solutions with C_i = 0.01, 0.02 M, at room temperature, in the manner stated above.

3. Results and discussion

3.1. Characterization of initial PGME and amino-functionalized samples

Copolymers with different epoxy group content (40 and 20 mass%, in PGME1 and PGME2, respectively) were synthesized by changing the amount of EGDMA. Non-porous PGME3 was prepared with the same amount of EGDMA as PGME1 (40 mass%), but without inert component. The samples were further functionalized with diethylene triamine. The amino groups concentrations calculated from the elemental analysis data were 5.01, 6.51 and 0.63 mmol g^{-1} in samples PGME1-deta, PGME2-deta and PGME3-deta, respectively [47].

The porosity parameters (specific pore volume, V_S, specific surface area, S_{Hg}, and pore diameter which corresponds to half of the pore volume, $d_{V/2}$) were calculated from the cumulative pore volume distribution curves [49] and presented in Table 1 (data taken from Ref. [47]), except for PGME3 and PGME3-deta. The non-porous nature of these two samples suggested that the more appropriate characterization technique was nitrogen physisorption that enables detection of smaller pores than mercury porosimetry. The results of nitrogen physisorption confirmed the absence of any porous structure since $S_{BET} < 1\ m^2\ g^{-1}$ for both PGME3 and PGME3-deta.

Pore volume is nearly the same for all porous samples but differences in pore distribution are significant. The increase of GMA content in the monomer mixture causes a shift in the pore size distribution curves of the synthesized samples toward larger pores, which led to the decrease in the specific surface area.

The surface morphology and bulk structure were investigated by scanning electron microscopy (Fig. 1). Porous copolymer beads of PGME1-deta (Figs. 1a–c) and PGME2-deta (Figs. 1d–f) had a coarse surface, due to the pores formed during the copolymerization process, while non-porous PGME3-deta (Figs. 1g–i) had a smooth and featureless surface. The non-porous beads had an almost ideal spherical shape (Fig. 1g), while the porous ones (Figs. 1a and d) showed certain irregularities.

The cross-section of the samples exposed distinctions between porous and non-porous beads. The porous beads, regardless of GMA/EGDMA ratio, had pores developed in the gaps between globular agglomerated structures. Somewhat smaller globes detected in Fig. 1c in comparison to Fig. 1f resulted in a more developed surface and therefore higher SHg of PGME1-deta in comparison to PGME2-deta. No pores were identified in the cross-sections of the non-porous samples (Figs. 1h and i). Only brittle fracture appearance, which is characteristic of non-porous epoxy polymers was observed [51].

3.2. Chromium(VI) sorption on amino-functionalized PGME

The binding mechanism of chromium(VI) to ion-exchange materials depends largely on its solution chemistry. Aqueous

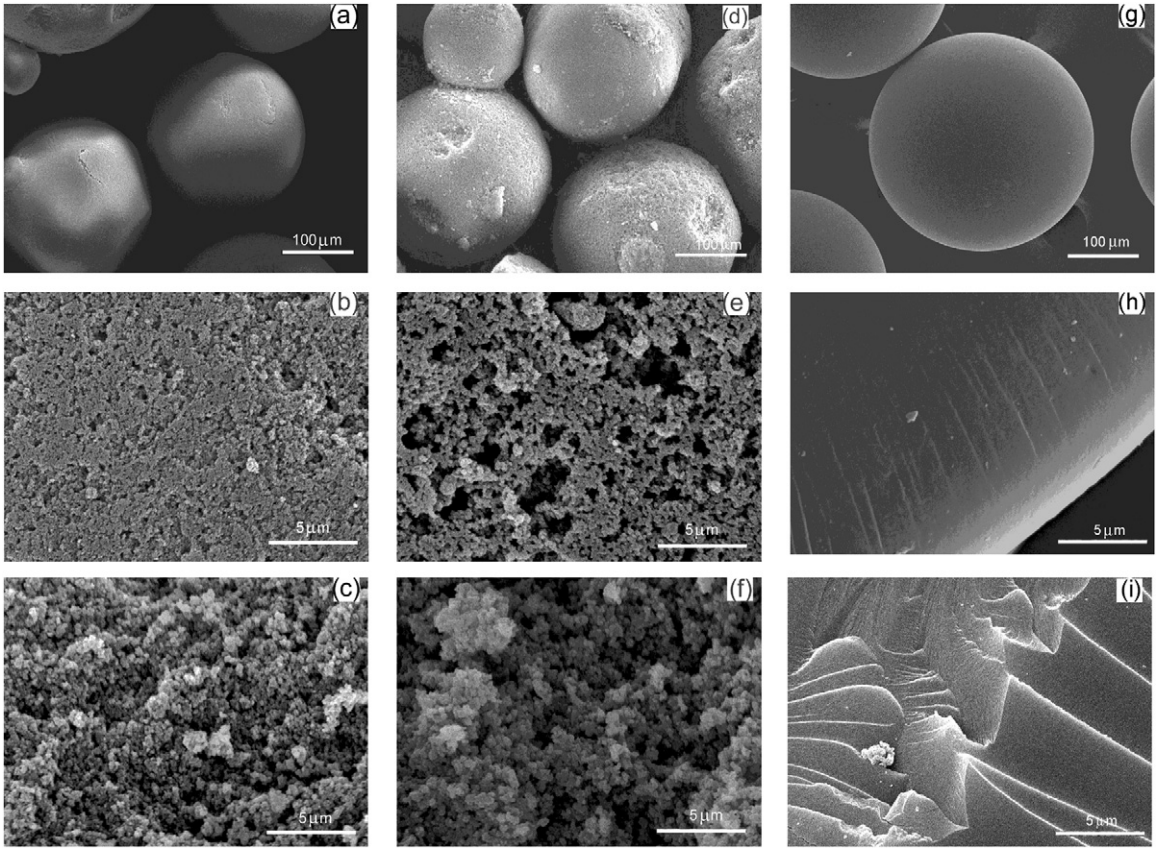

Fig. 1. SEM micrographs: PGME1-deta beads (a), surface (b), cross-section (c), PGME2-deta beads (d), surface (e), cross-section (f), PGME3-deta beads (g), surface (h), and cross-section (i).

solution pH affects the speciation of chromium and the surface charge of the adsorbent [52]. At pH 1.0, chromium ions exist in the form of chromic acid (H_2CrO_4), while in the pH range 2.0–6.0 different forms of chromium ions such as dichromate ($Cr_2O_7^{2-}$), hydrochromate ($HCrO_4^-$), and polychromates ($Cr_3O_{10}^{2-}$, $Cr_4O_{13}^{2-}$) coexist, of which $HCrO_4^-$ predominates. With further pH increase, this form shifts to CrO_4^{2-} and $Cr_2O_7^{2-}$ [53]. $Cr_2O_7^{2-}$ is dimmer of $HCrO_4^-$ which is formed when the concentration of chromium exceeds ~1 g L^{-1}. Thus, the most active chromium(VI) species under acidic conditions are $Cr_2O_7^{2-}$, $HCrO_4^-$ and CrO_4^{2-}.

The two foremost means of interaction of an anion exchange resin and ions involve ion-exchange and chelation of metal ions. These interactions depend on the resin structure in terms of present functional groups. The amino groups (—NH_2) of PGME-deta would be in protonated cationic form (—NH_3^+) to a high extent in acidic solution. This makes the resin surface positively charged and electrostatic interaction occurs between the sorbent and chromate anions resulting in superior chromium uptake [21].

In our recent work on pertechnetate sorption with PGME-deta, it was proposed that non-specific sorption of pertechnetate anion via electrostatic interaction takes place at the protonated amino groups of macroporous crosslinked PGME [47]. By analogy, hydrochromate anion (dominant species at pH 1.8) sorption would likely proceed by the same mechanism.

It was established in our earlier study that pH 1.8 was optimal for maximum Cr(VI) removal by PGME-deta [46,50], thus the majority of experiments in this study were performed at this pH value. The protonated form of the amino groups of the copolymer is prevalent at pH 1.8, and the principal if not the only present form of chromium in the solution are chromate and dichromate anions; this deduction is further supported by literature data [1,21]. The amino groups (—NH_2) of the copolymer in acidic solution would be in the protonated cationic form (—NH_3^+) to a high degree resulting in stronger attraction for negatively charged ions in the solution. Electrostatic interaction occurs between the adsorbent and anions resulting in high chromium removal. Presumed mechanism is presented in Scheme 1 where $HCrO_4^-$ was chosen as representative anion.

The presence of primary and secondary amino groups in the functionalized copolymer structure categorize it as a weak base anion exchange resin. The pK_a values of such amino groups are in the range of 8–10 [54]. Thus, a number of amino groups remain in their protonated form even at circumneutral pH values. In regard to this, several experiments were performed to estimate the kinetics and the sorption capacity at unadjusted solution pH (3.8), and the results will be discussed separately.

The maximum experimental uptake values for PGME1-deta, PGME2-deta and PGME3-deta were found to be 2.48, 2.68 and 0.44 mmol g^{-1} at 25 °C, respectively, significantly lower than the concentration of amino groups on the resins [50]. This may be

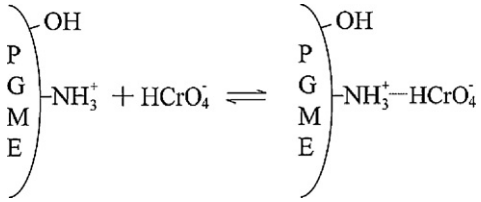

Scheme 1. Presumed mechanism of interaction between adsorbent (PGME-deta) and adsorbate.

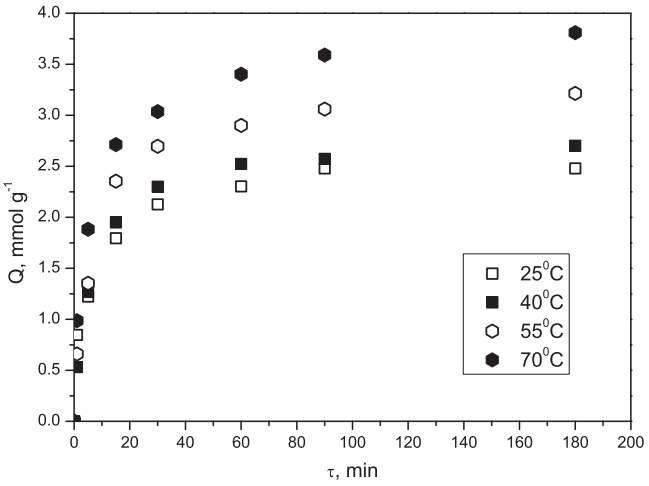

Fig. 2. Effect of temperature on Cr(VI) adsorption rate on PGME1-deta (C_i = 0.1 M).

ascribed to the relatively large size of chromium(VI) anionic species, steric hindrances in interactions with amino group sites caused by the rigid macroporous structure of copolymers, and mass transfer resistance. At 55 and 70 °C, the maximum experimental sorption capacity for PGME1-deta significantly increases to 3.21 and 3.81 mmol g^{-1}, respectively, due to an increase in diffusion and ligand chain mobility. However, these temperature conditions lean toward the extreme, and particularly difficult for application.

The effect of temperature on Cr(VI) ions removal by PGME1-deta was investigated in the temperature range 25–70 °C, as a function of contact time. The results are given in Fig. 2. The temperature rise promotes Cr(VI) removal and brings about an increase in the initial rate of adsorption. The maximum experimental sorption capacity of PGME1-deta was 198 mg g^{-1}.

3.3. Kinetic models

Determination of the rate at which Cr(VI) removal takes place in the used solid/solution system is one of the crucial factors for the effective design of the sorption system [55]. In order to examine the controlling mechanism of sorption processes, such as mass transfer and chemisorption, five kinetic models were used to test the experimental data, i.e. the pseudo-first, the pseudo-second order, Elovich equation, intraparticle diffusion and Bangham model. Kinetic data for Cr(VI) sorption on PGME-deta was collected for various Cr(VI) initial concentrations (pH = 1.8, 3.8; t = 25 °C), and at different temperatures (for PGME1-deta at pH = 1.8, C_i = 0.1 M).

The experimental kinetic data were treated with the models given in Table 2. Kinetic parameters calculated for five kinetic models are collected in Tables 3 and 4. As an illustration, plots for the pseudo-first, the pseudo-second order and Elovich model for Cr(VI) sorption by PGME2-deta were shown in Fig. 3. and for intraparticle and Bangham diffusion in Fig. 4.

The pseudo-first order kinetic model is not applicable since R^2 values were rather low. The theoretical Q_e^{calc} values calculated from

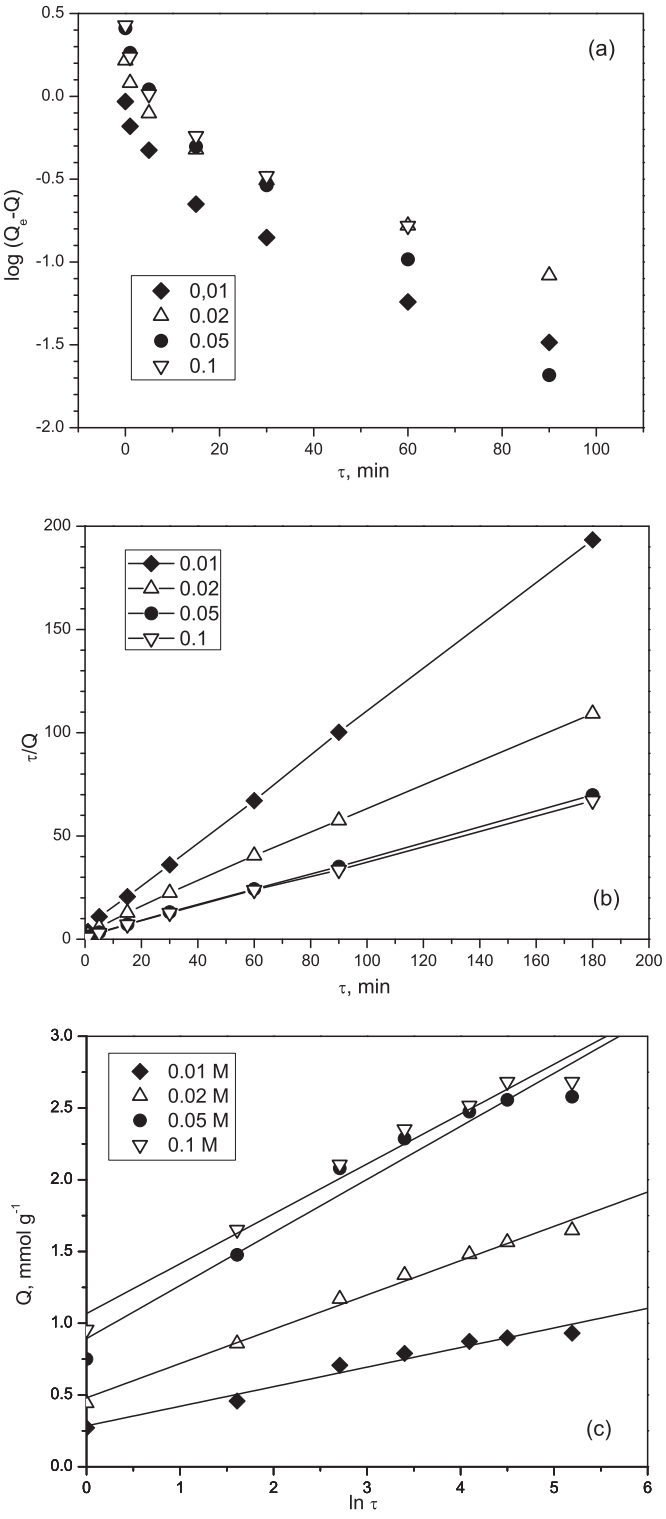

Fig. 3. Pseudo-first (a) pseudo-second order kinetics (b) and Elovich plots (c) of Cr(VI) uptake by PGME2-deta (pH = 1.8, t = 25 °C).

Table 2
Kinetic models.

Kinetic model	Equation	References
Pseudo-first-order	$\log(Q_e - Q_t) = \log Q_e - \left(\frac{k_1 \tau}{2.303}\right)$	[56]
Pseudo-second-order	$\frac{\tau}{Q} = \frac{1}{k_2 Q_e^2} + \frac{1}{Q_e}\tau$ $h = k_2 Q_e^2$	[55]
Elovich equation	$Q = \frac{\ln a_e b_e}{b_e} + \frac{1}{b_e} \ln \tau$	[57]
Intraparticle diffusion	$Q = C_{id} + k_{id} \cdot \tau^{0.5}$	[58,59]
Bangham diffusion	$\log \log \left[\frac{C_i}{C_i - C_s Q}\right] = \log \left[\frac{k_b C_s}{2.303 V}\right] + \alpha \log \tau$	[60]

pseudo-second order model are very close to the experimental Q_e values, with $R^2 \geq 0.998$. Eventhough R^2 values for Elovich model were poorer than for the pseudo-second order, they were still rather high. The correlation for PGME3-deta was especially poor (R^2 = 0.62–0.87), attributable to the fact that sorption is restricted to the easily accessible surface of the beads. The sorption process is complete after a short time period, which in turn renders the Elovich equation inadequate for modeling the sorption on

Table 3
Kinetic parameters for Cr(VI) using PGME-deta as adsorbent (pH = 1.8, t = 25 °C) [50].

	PGME1-deta				PGME2-deta				PGME3-deta			
	C_i, M											
Q_e, mmol g^{-1}	0.01	0.02	0.05	0.1	0.01	0.02	0.05	0.1	0.01	0.02	0.05	0.1
	0.93	1.63	2.37	2.48	0.93	1.65	2.58	2.68	0.11	0.25	0.41	0.44
Pseudo-first order												
k_1, min^{-1}	0.034	0.039	0.050	0.041	0.035	0.030	0.051	0.045	0.104	0.122	0.246	0.449
Q_e^{calc}, mmol g^{-1}	0.38	1.13	1.68	1.66	0.57	1.05	1.81	1.79	0.10	0.23	0.37	0.44
R^2	0.921	0.962	0.983	0.902	0.871	0.915	0.962	0.862	0.989	0.988	0.950	0.990
Pseudo-second order												
k_2, g mmol^{-1} min^{-1}	0.194	0.102	0.088	0.081	0.249	0.112	0.113	0.113	2.42	1.42	2.85	3.69
h, mmol g^{-1} min^{-1}	0.18	0.29	0.52	0.53	0.22	0.32	0.78	0.84	0.03	0.09	0.43	0.73
Q_e^{calc}, mmol g^{-1}	0.96	1.68	2.43	2.55	0.95	1.68	2.63	2.73	0.11	0.26	0.41	0.44
R^2	0.999	0.999	0.999	0.999	0.999	0.999	0.999	0.999	0.999	0.999	0.999	0.999
Elovich												
a_e, mmol g^{-1} min^{-1}	1.22	1.31	2.47	3.58	1.37	1.63	2.46	2.90	0.0715	0.284	2.91	1.88
b_e, g mmol^{-1}	7.57	3.92	2.78	2.85	7.32	4.18	2.78	2.88	54.8	25.1	20.2	12.8
R^2	0.965	0.969	0.949	0.963	0.962	0.988	0.943	0.964	0.866	0.860	0.749	0.616
Intraparticle												
k_{id}, mmol g^{-1} min$^{-0.5}$	0.051	0.080	0.100	0.115	0.034	0.069	0.101	0.104	[a]			
C_{id}, mmol g^{-1}	0.48	0.91	1.45	1.41	0.59	0.93	1.17	1.73				
R^2	0.966	0.965	0.939	0.932	0.933	0.963	0.967	0.912				
Bangham												
$k_b \cdot 10^3$, g^{-1}	1.76	1.28	0.0817	0.467	1.67	1.43	1.00	0.582	[a]			
α	0.409	0.402	0.303	0.243	0.429	0.374	0.290	0.220				
R^2	0.981	0.969	0.929	0.949	0.979	0.974	0.893	0.912				

[calc] –calculated from pseudo-first, i.e. pseudo-second order model linear fit equation.
[a] Not applicable.

PGME3-deta for longer sorption times [61]. Overall, the initial sorption rates h and a_e, increase with the ascending initial concentration as expected.

The superior fit of the pseudo-second-order model with experimental data implies that the adsorption process is surface-reaction controlled, with chemisorptions involving valence forces through sharing or exchange of electrons between PGME-deta and chromium(VI) species [62]. The fact that R^2 values for Elovich model were rather high corroborates the assumption that chemisorption is the main adsorption controlling mechanism.

The previously observed initial rapid chromium sorption within the first 30 min, with the uptake capacity higher than 80% [46,50] suggests that more than one mechanism may also be involved in the process. Since the pseudo-first, the pseudo-second order and Elovich kinetic models cannot identify the influence of diffusion on sorption; Weber and Morris' equation and Bangham's model were used.

The dependence of the amount adsorbed on the square-root of time has a concave character for the two copolymers (Fig. 4a). A model investigation by Rudzinski et al. has shown that such curve shape may be due to a combined effect of the rate of surface reaction and that of the solute transport from the bulk to the surface [61]. The plots Q_τ vs. $t^{1/2}$ did not pass through the origin suggesting that even though the adsorption process involved intraparticle diffusion, it was not the only rate-controlling step [63]. The positive value of C_{id} is indicative of some degree of boundary layer control [64]. The kinetic data for sorption of Cr(VI) on non-porous PGME3-deta was not treated with diffusion models, since these are inapplicable.

The plots have first sharper portion (Fig. 4a), which can be considered as an external surface adsorption or faster adsorption stage, followed by gradual adsorption where intraparticle diffusion is rate controlled. In the final equilibrium stage the intraparticle diffusion starts to slow down due to the lower adsorbate concentration in solution.

Kinetic data for porous sorbents were further used to confirm pore diffusion as one of the rate-controlling steps using Bangham's equation. If this equation is an adequate representation of experimental data, than the adsorption kinetics is limited by pore diffusion [60]. The Bangham's model did not strictly match experimental data verifying again that the diffusion into the pores of the sorbent was of consequence, but not the sole rate-determining process.

3.4. Adsorption isotherms

Adsorption equilibrium, usually described by an isotherm equation whose parameters express the surface properties and affinity of the sorbent (at a fixed temperature and pH), together with the sorption kinetics, provide fundamental physicochemical data for

Table 4
Kinetic parameters for Cr(VI) using PGME1-deta as adsorbent (pH = 1.8, C_i = 0.1 M).

t, °C	25	40	55	70
Q_e, mmol g^{-1}	2.48	2.70	3.21	3.81
Pseudo-first order				
k_1, min^{-1}	0.041	0.033	0.031	0.030
Q_e^{calc}, mmol g^{-1}	1.66	1.73	2.12	2.01
R^2	0.902	0.885	0.900	0.921
Pseudo-second order				
k_2, g mmol^{-1} min^{-1}	0.081	0.061	0.047	0.040
h, mmol g^{-1} min^{-1}	0.53	0.47	0.51	0.61
Q_e^{calc}, mmol g^{-1}	2.55	2.78	3.31	3.91
R^2	0.999	0.999	0.999	0.998
Elovich				
a_e, mmol g^{-1} min^{-1}	3.58	1.82	2.03	3.61
b_e, g mmol^{-1}	2.85	2.27	1.91	1.78
R^2	0.963	0.964	0.960	0.988
Intraparticle				
k_{id}, mmol g^{-1} min$^{-0.5}$	0.115	0.109	0.120	0.157
C_{id}, mmol g^{-1}	1.41	1.61	1.95	2.04
R^2	0.932	0.898	0.944	0.980
Bangham				
$k_b \cdot 10^3$, g^{-1}	0.467	0.350	0.413	0.606
α	0.243	0.336	0.341	0.295
R^2	0.949	0.891	0.944	0.940

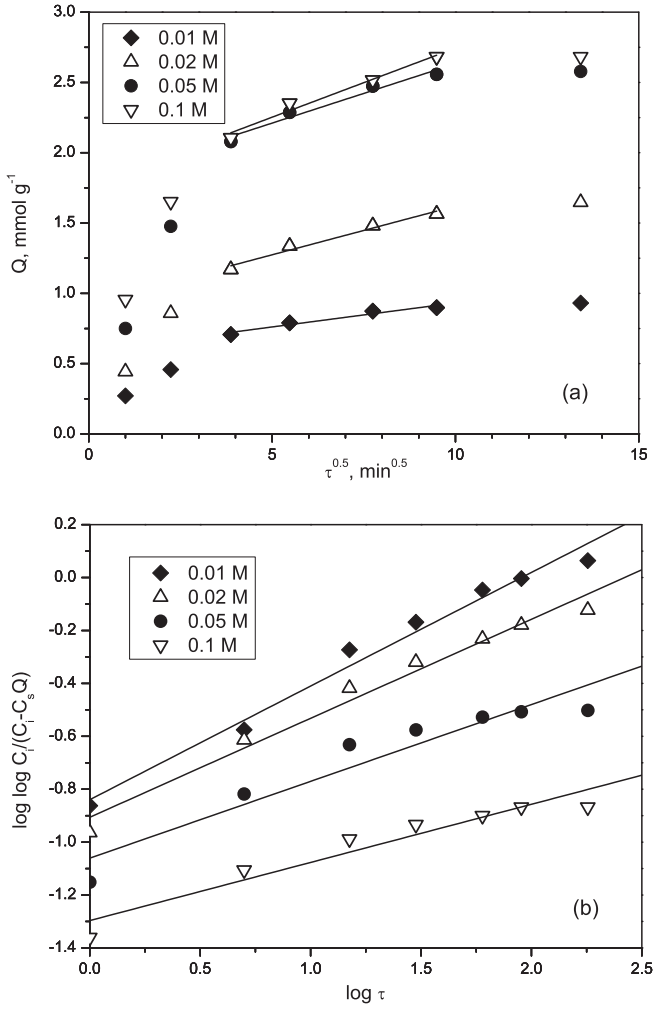

Fig. 4. Intraparticle (a) and Bangham (b) diffusion plots for Cr(VI) adsorption on PGME2-deta (pH = 1.8, t = 25 °C).

evaluating the applicability of an adsorption process as a unit operation [65]. The equilibrium adsorption data presented in Fig. 5 were fitted with Langmuir, Freundlich and Tempkin equations (Table 5). Isotherm parameters and regression data for Cr(VI) sorption on PGME-deta samples at 25 °C were presented in Table 6.

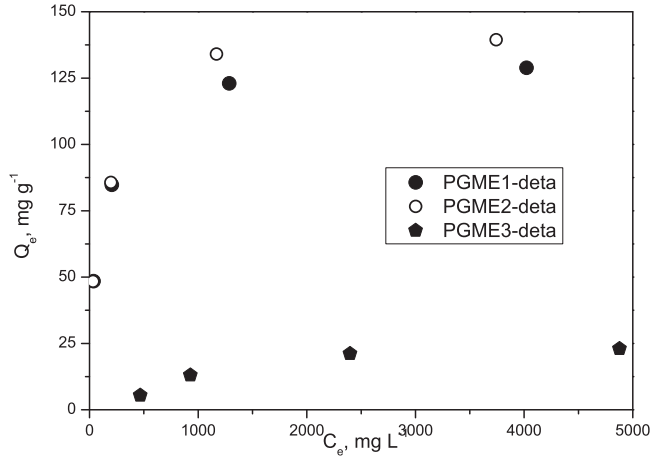

Fig. 5. Adsorption isotherms for Cr(VI) sorption on PGME-deta samples (t = 25 °C).

Table 5
Isotherm models.

Isotherm models	Linearized equation	Reference
Langmuir	$\frac{C_e}{Q_e} = \frac{1}{Q_{max}K_L} + \frac{C_e}{Q_{max}}$	[66]
Freundlich	$\ln Q_e = \ln K_F + \frac{1}{n}\ln C_e$	[67]
Tempkin	$Q_e = \frac{RT}{b_T}\ln K_T + \frac{RT}{b_T}\ln C_e$	[23,68]

The experimental data obtained for the porous sorbents conformed best by far to the Langmuir model based on R^2 values (Table 6), indicating homogeneous distribution of active sites on PGME-deta and monolayer sorption. For non-porous PGME3-deta Langmuir model was only marginally better than Tempkin. Freundlich isotherm does not represent the equilibrium data satisfactorily for all samples.

3.5. Comparison with other adsorbents

The literature data on hexavalent chromium removal include various adsorbents, like activated carbons, low cost adsorbents (lignite, peat, chars, coals), clay minerals, industrial waste/by-products (fly ash, waste sludges, mud, lignin), biosorbents (algae, fungi, bacteria, plants, peat, chitin, chitosan), commercial ion-exchange resins, polymers (natural or synthetic), etc. [69]. To justify the practicability of the presented materials as effective Cr(VI) removing agents, the adsorption capacities of PGME-deta need to be compared to those of other adsorbents. Table 7 gives an overview of some adsorbents focusing on the results published in the past two years.

Discrepancies in the experimental conditions render direct comparison of the literature data nearly impossible. Just for the sake of comparison, we will mention some of those results.

The maximum adsorption capacity, Q_{max}, has been widely used to compare the efficiency of an absorbent. The Q_{max} of adsorbents listed in Table 7, lie in a wide range between 0.05 mg g^{-1} reported for volcanic rocks [70] up to approximately 350 mg g^{-1} for PEI-modified aerobic granular sludge [76] and wheat straw functionalized with DETA [27].

The maximum monolayer capacities obtained for PGME-deta samples, calculated from the Langmuir isotherm were found to be 132 mg g^{-1}, 143 mg g^{-1} and 25.6 mg g^{-1} for PGME1-deta at 25 °C, PGME2-deta and PGME3-deta, respectively (Table 6). Porous PGME-deta exhibits sorption capacities even superior to the majority of the recently reported sorbent types, while it is among the cheapest and most easily obtained.

The Langmuir isotherm and the pseudo-second order kinetic model were shown to be the most suitable for fitting experimental data in the papers cited in Table 7 as was the case with our results.

Table 6
Isotherm parameters and regression data for Cr(VI) sorption on PGME-deta samples at 25 °C.

Models	Parameters	Samples		
		PGME1-deta	PGME2-deta	PGME3-deta
Langmuir	Q_{max}, mg g^{-1}	132	143	25.6
	K_L, L g^{-1}	11.41	10.95	0.580
	R_L	0.0166	0.0173	0.932
	R^2	0.999	0.999	0.913
Freundlich	n	4.73	4.34	1.67
	$1/n$	0.211	0.231	0.599
	K_F, (mg g^{-1})/(mg L^{-1})$^{1/n}$	24.83	23.46	0.171
	R^2	0.908	0.923	0.812
Tempkin	B_T	17.8	20.3	7.63
	K_T, L mg^{-1}	0.510	0.367	0.00512
	R^2	0.971	0.968	0.903

Table 7
Overview of Cr(VI) uptake with various adsorbents.

Sorbent	pH	t, °C	C_i range, mg L^{-1}	C_i, mg L^{-1}	Isotherm model	Kinetic model	Q_{max}[a], mg g^{-1}	References
Volcanic rocks-pumice	2.0	25	0.5–10.0	10.0	L	Pseudo-second	0.046	[70]
Hematite	8.0	25	0.1–16	–	L	–	2.299	[28]
Goethite							1.955	
α-Alumina							2.158	
Titanium oxide–Ag composite	2.0	25	30–80	40	L	Pseudo-second	25.7	[71]
(3-Mercaptopropyl) trimethoxysilane functionalized acid-activated sepiolite	3 .0	25	5–100	100	D-R	–	7.732	[72]
HDTMA-modified Pohang clinoptilolite	3.0	20	32–225	–	L	Pseudo-second	3.55	[73]
HDTMA-modified Haruna chabazite							8.83	
Sawdust	1.0	30	50–500	500	L	Pseudo-second	41.52	[23]
Newspapers	1.0	30	–	100	F, R-P	Pseudo-second	55.06	[74]
Alligator weed	1.0	50	160–360	320	L	Pseudo-second	88.11	[24]
Daucus carota L. waste biomass	5.0	30	25–800	110	L	Pseudo-second	88.27[b]	[25]
Rice bran	2.0	30	5–300	–	L	Pseudo-second	12.341	[26]
Neem leaves							15.954	
Coconut shell							18.695	
Surface modified tannery residual biomass	2.0	50	100–350	350	L	Pseudo-second	217.39	[75]
PEI-modified aerobic granular sludge	5.2	20	10–500	–	R-P	–	348.125	[76]
Wheat straw functionalized with DETA	5.0	30	150–350	350	F	Pseudo-second	322.58	[27]
Starch functionalized with EDA	4.0	25	14–48	–	F	Pseudo-second	15.17	[30]
Chitosan coated with poly 3-methyl thiophene	2.0	25	50–200	200	L	Pseudo-second	127.62	[19]
Quaternary amine modified magnetic crosslinked chitosan resin	8.0	45	–	260	L	Pseudo-second	179[c]	[20]
Cross-linked magnetic chitosan resin functionalized with EDA	2.0	20	20–200	200	L, T	Pseudo-second	51.813	[21]
Bio-char (oakbark)	2.0	45	1–100	–	S	Pseudo-second	7.51	[77]
H_3PO_4-activated lignin	2.0	20	5–50	100	K-C	Pseudo-second	77.85	[78]
Fe-modified activated carbon	6.0	20	3.5–20	20	T, F	Pseudo-second	11.83	[79]
poly(4-VP-*co*-DVB) functionalized with 2-chloroacetamide	3.0–5.0	45	5–1000	1000	L, F	Reversible first-order	94.34	[31]
Quaternized crosslinked poly(4-VP)	Initial pH	30	5–1000	–	F	Reversible first-order	142.85	[32]
Cr(VI)-imprinted poly(4-VP-*co*-2-HEMA)	4.0	25	20–400	200	L	Pseudo-second	178[b] calc	[33]
P(EGMA-*co*-VI)	3.0	25	100–3000	3000	–	–	109[b]	[5]
Aminolyzed VAc/AN/DVB terpolymer, quaternized with 2-chloroacetone	1.5	20	500–2000	2000	L	Pseudo-second	188.6	[17]
Fe_3O_4 coated PPy	2.0	55	200–600	600	L	Pseudo-second	238.09	[34]
PANI/PEG composite	5.0	25	10–100	100	L, F	–	109.9	[35]
PGMA grafted MRS, functionalized with EDA	5	25	21–130	130	L	–	156	[36]
Amino-functionalized poly(GMA-*co*-EGDMA)	1.8	25	–	2600	–	Pseudo-second	110[b]	[46]
Magnetic MMA/GMA/DVB terpolymer functionalized with EDA	2.5	35	10–150	150	L	Pseudo-second	61.35	[37]
PGME1-deta	1.8	25	520–5200	5200	L	Pseudo-second	132	This study
PGME2-deta							143	

Where: L – Langmuir model, F – Freundlich, D-R –Dubinin-Radushkevich model, R-P – Redlich-Peterson model, S – Sips model, K-C – Koble–Corrigan model. HDTMA – hexadecyltrimethylammonium bromide; PEI – poly(ethylene imine); DETA – diethylene triamine; EDA – ethylene diamine; poly(4-VP-*co*-DVB) – poly(4-vinylpyridine-*co*-divinylbenzene); 2-HEMA – 2-hydroxyethyl methacrylate; P(EGMA-*co*-VI) – poly(ethylene glycol methacrylate-*co*-vinyl imidazole); VAc/AN/DVB – poly(vinyl acetate-*co*-acrylonitrile-*co*-divinyl benzene) terpolymer; PPy – poly(pyrrole); PANI – poly(aniline); PEG – poly(ethylene glycol); PGMA – poly(glycidyl methacrylate); MRC – Merrifield chloromethylated resin; MMA – methyl methacrylate.

[a] Monolayer capacity, calculated from Langmuir isotherm.
[b] Maximal capacity, calculated from experimental data.
[c] Calculated from mmol g^{-1}.

3.6. Effect of temperature and thermodynamic studies

Thermodynamic considerations of an adsorption process are necessary to establish whether the process is spontaneous and feasible or not. The employed equations are listed in Table 8.

The experimental data obtained for Cr(VI) adsorption on the representative PGME1-deta at various temperatures were used for calculating the thermodynamic parameters given in Table 9.

The activation energy for the adsorption system of Cr(VI) onto PGME1-deta was found as 15.8 kJ mol^{-1}. As known when the rate is controlled by intraparticle diffusion mechanism, the activation energy is low and within the range of values of 8–22 kJ mol^{-1} for ion-exchange, diffusion-controlled processes [82].

The negative value of ΔG indicates that the adsorption of Cr(VI) onto PGME1-deta is feasible and spontaneous, without induction period [83], and that the processes are favorable for the formation of electrostatic interaction and/or chromium–adsorbent complexes [1]. The value of ΔG became slightly more negative with rise of

Table 8
Thermodynamics equations.

Apparent equilibrium constant equation	$\log K_c = \frac{F_e}{1-F_e}$	[80]
Van't Hoff equation	$\log K_c = \frac{\Delta S}{2.303R} - \frac{\Delta H}{2.303RT}$	[80]
Arrhenius equation (linearized)	$\ln k_2 = \ln A - \frac{E_a}{RT}$	[81]

Table 9
Thermodynamic parameters for Cr(VI) sorption onto PGME1-deta.

t, °C	ΔG, kJ mol^{-1}	E_a, kJ mol^{-1}	$T\Delta S$, kJ mol^{-1}	$-\Delta H$, kJ mol^{-1}
25	−1.46	15.8	19.8	18.3
40	−2.39		20.7	
55	−3.19		21.6	
70	−4.26		22.5	

Table 10
Kinetic parameters for Cr(VI) using PGME-deta as adsorbent (pH = 1.8, t = 25 °C).

C_i, M	0.01	0.02
$Q_{e\ exp}$, mmol g^{-1}	0.53	1.02
Pseudo-first order		
k_1, min^{-1}	0.042	0.041
Q_e, mmol g^{-1}	0.35	0.67
R^2	0.963	0.963
Pseudo-second order		
k_2, g mmol^{-1} min^{-1}	0.383	0.195
h, mmol g^{-1} min^{-1}	0.11	0.21
Q_e, mmol g^{-1}	0.55	1.05
R^2	0.999	0.999
Elovich		
a_e, mmol g^{-1} min^{-1}	0.709	1.46
b_e, g mmol^{-1}	13.0	6.92
R^2	0.940	0.949
Intraparticle		
k_{id}, mmol g^{-1} min$^{-0.5}$	0.023	0.042
C_{id}, mmol g^{-1}	0.32	0.62
R^2	0.913	0.953
Bangham		
$k_b \cdot 10^3$, g^{-1}	1.03	0.990
α	0.284	0.276
R^2	0.933	0.969

temperature, indicating improved adsorption at higher temperatures. The positive ΔH value indicates that Cr(VI) adsorption onto PGME1-deta is an endothermic process, and since the sorption capacity increases with temperature, one can say that chemisorption process is significant and rate controlling. The positive ΔS value indicates an increase in randomness at the solid/solution interface during the adsorption of Cr(VI) adsorption onto PGME1-deta [1]. Water molecules are released from the hydrated Cr(VI) anions or from the surface, gaining more translational entropy than is lost by the adsorbate ions, thus allowing the prevalence of randomness in the system [84]. The entropy contribution at studied temperatures is sufficient to prevail over the opposite enthalpy contribution to ΔG, causing its value to be negative, thus making the sorption process spontaneous.

3.7. Sorption at unadjusted pH

pH regulation in sizeable volumes of wastewater during one or more stages of refining may not always be practicable or desirable. In order to examine sorption dynamics under such conditions, kinetic data for Cr(VI) sorption on one PGME-deta sample (PGME1-deta) at unadjusted pH were also tested with kinetic models. Relevant kinetic parameters, as well as regression coefficients R^2 were listed in Table 10.

The removal efficiency was 72% for C_i = 0.01 M and 61% for C_i = 0.02 M suggesting that porous PGME-deta may be employed in the pretreatement stages of purification to drastically reduce Cr(VI) concentration. The Q_e values for 0.01 M and 0.02 M Cr(VI) solutions were 0.53 mmol g^{-1} and 1.02 mmol g^{-1}, considerably less than at pH 1.8 when the sorbent performance is maximal. The pseudo-second-order and Elovich initial sorption rates show that the process is much slower at pH 3.8. The slopes of intraparticle diffusion plots are less steep, revealing that diffusion into the pores has slowed down compared to the experiments performed at pH 1.8. The Bangham parameters support this claim and the explanation lies in decreased percentage of protonated amino groups and increase in neutral chromium(VI) species.

For further understanding of Cr(VI) removal microscopic analysis was performed on PGME1-deta after unfavorable sorption. Fig. 6 shows TEM and SEM micrographs of PGME1-deta after the Cr(VI) sorption experiment on unadjusted pH = 3.8. The EDS analysis was

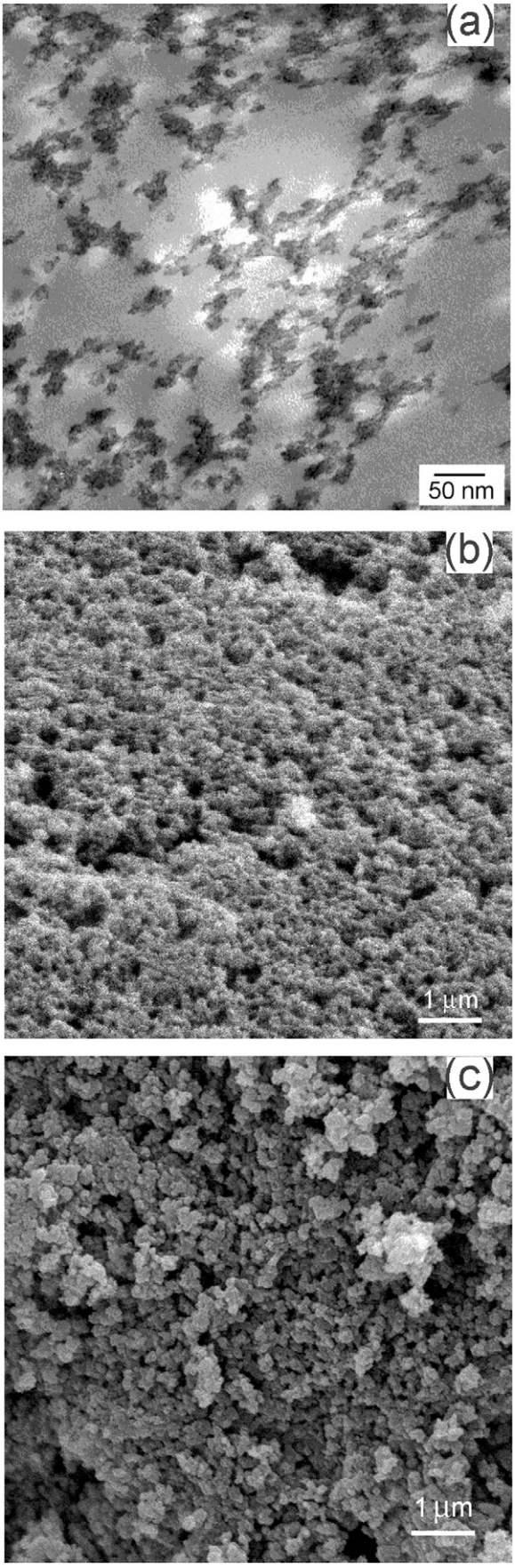

Fig. 6. Microphotographs of PGME1-deta after sorption; C_i = 0.02 M, pH = 3.8, t = 25 °C: TEM (a), SEM of surface (b), and SEM of cross-section (c).

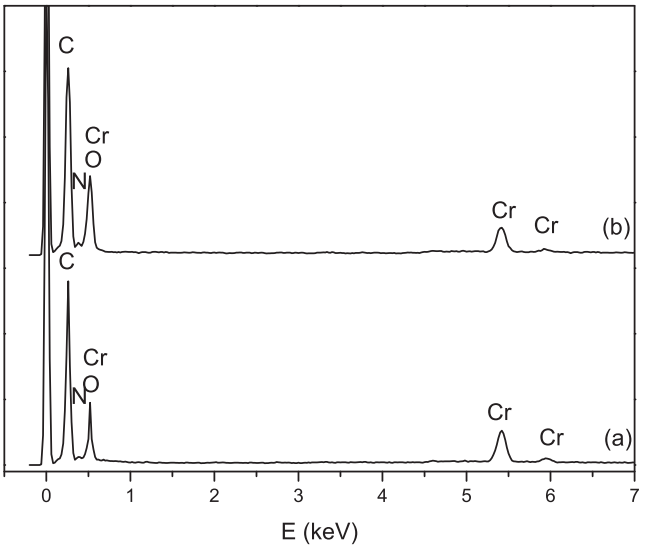

Fig. 7. EDS spectra of PGME1-deta after Cr(VI) sorption: surface of bead (a) and cross-section (b).

performed on both surface of PGME1-deta bed (Fig. 6b) and on its cross-section (Fig. 6c) and given in Fig. 7.

TEM image demonstrates that chromium is evenly dispersed throughout the copolymer. The particular appearance is due to patchy ligand distribution. The SEM microphotograps confirmed the preserved porous structure after the sorption process.

On EDS spectra C, O, N and Cr were identified. EDS analysis proved that a significant amount of chromium binds to the sites on the interior surface (Fig. 7a) of the beads (3.1 mass%) as well as on the exterior (Fig. 7b) (5.7 mass%) even at low concentrations and unfavorable pH.

4. Conclusion

Two porous and one non-porous poly(GMA-*co*-EGDMA) sample were synthesized by suspension copolymerization and functionalized with diethylene triamine. The possibility of Cr(VI) removal from aqueous solutions was tested under non-competitive conditions. Kinetics of Cr(VI) sorption was tested in the temperature range 25–70 °C and analyzed using pseudo-first order, pseudo-second order, Elovich, intraparticle diffusion and Bangham model. Kinetic studies showed that the adsorption adhered to the pseudo-second-order model since theoretical and experimental sorption capacities were in excellent agreement and $R^2 \geq 0.998$. Elovich model confirmed that chemisorption is the main adsorption controlling mechanism. The intraparticle diffusion model revealed that pore diffusion was not the only rate-controlling step and indicated some degree of boundary layer control in the process of Cr(VI) sorption by the porous copolymer. Bangham's model confirmed that these sorption processes were diffusion controlled.

The equilibrium isotherm study showed the best suitability of Langmuir model for the investigated system, indicating homogeneous distribution of active sites by the PGME-deta and monolayer sorption. The maximum monolayer sorption capacities at pH 1.8 and 25 °C were 132 mg g^{-1} and 143 mg g^{-1} for porous PGME-deta and 25.6 mg g^{-1} for non-porous. These findings are comparable with or better than the literature data. Generally, the sorbents more efficient than porous PGME-deta were those that are inappropriate for column packing applications and regeneration which will be the subject of further experiments.

Thermodynamic parameters revealed that the Cr(VI) adsorption onto PGME-deta was endothermic and spontaneous, with increased randomness in the system. The temperature rise promotes Cr(VI) removal and brings about an increase in the initial rate of adsorption. The maximum experimental sorption capacity was 198 mg g^{-1} at 70 °C.

Our findings promote macroporous amino-functionalized PGME as potentially very efficient and cost-effective hexavalent chromium adsorbent.

Acknowledgements

This work was supported by the Ministry of Education and Science of the Republic of Serbia (Projects III 43009, III 45001 and ON 172018).

The authors are most grateful to University of Groningen, Zernike Institute for Advanced Materials, Polymer Chemistry Department, The Netherlands for being able to use the TEM, particularly to M.Sc. Ivana Vuković, for her assistance.

References

[1] G. Bayramoglu, M.Y. Arica, Adsorption of Cr(VI) onto PEI immobilized acrylate-based magnetic beads: isotherms, kinetics and thermodynamics study, Chem. Eng. J. 139 (2008) 20–28.
[2] N.N. Greenwood, A. Earnshaw, Chemistry of the Elements, Butterworth Heinemann, Oxford, 1998, pp. 1002–1039.
[3] I. Narin, Y. Surme, M. Soylak, M. Dogan, Speciation of Cr(III) and Cr(VI) in environmental samples by solid phase extraction on Ambers orb 563 resin, J. Hazard. Mater. 136 (2006) 579–584.
[4] P.A. Kumar, M. Ray, S. Chakraborty, Adsorption behaviour of trivalent chromium on amine-based polymer aniline formaldehyde condensate, Chem. Eng. J. 149 (1–3) (2009) 340–347.
[5] E. Uğuzdoğan, E.B. Denkbas, O.S. Kabaşakal, The use of polyethyleneglycolmethacrylate-co-vinylimidazole (PEGMA-co-VI) microspheres for the removal of nickel(II) and chromium(VI) ions, J. Hazard. Mater. 177 (2010) 119–125.
[6] M.C. Graham, J.G. Farmer, Chemistry of freshwaters, in: R.M. Harrison (Ed.), Principles of Environmental Chemistry, RSC Publishing, Cambridge, 2007, pp. 80–169.
[7] M. Costa, Potential hazards of hexavalent chromate in our drinking water, Toxicol. Appl. Pharmacol. 188 (1) (2003) 1–5.
[8] World Health Organization, Chromium in Drinking-Water, Guidelines for Drinking-Water Quality, Vol. 2, Health Criteria and Other Supporting Information, 2nd ed., World Health Organization, Geneva, 1996.
[9] U.S. Environmental Protection Agency, Toxicological Review of Hexavalent Chromium, National Center for Environmental Assessment, Office of Research and Development, Washington, DC, 1998.
[10] P. Miretzkya, A. Fernandez Cirelli, Cr(VI) and Cr(III) removal from aqueous solution by raw and modified lignocellulosic materials: a review, J. Hazard. Mater. 180 (1–3) (2010) 1–19.
[11] D. Kaušpėdienė, E. Kazlauskienė, A. Gefenienė, R. Binkienė, Comparison of the efficiency of activated carbon and neutral polymeric adsorbent in removal of chromium complex dye from aqueous solutions, J. Hazard. Mater. 179 (1–3) (2010) 933–939.
[12] R. Codd, C.T. Dillon, A. Levina, P.A. Lay, Studies on the genotoxicity of chromium: from the test tube to the cell, Coord. Chem. Rev. 537 (2001) 216–217.
[13] A. Baran, E. Bıçak, Ş.H. Baysal, S. Önal, Comparative studies on the adsorption of Cr(VI) ions on to various sorbents, Bioresour. Technol. 98 (2006) 661–665.
[14] R.R. Patterson, S. Fendorf, M.J. Fendorf, Reduction of hexavalent chromium by amorphous ion sulfide, Environ. Sci. Technol. 31 (1997) 2039–2044.
[15] A. Bódalo, J.L. Gómez, E. Gómez, A.M. Hidalgo, A. Alemán, Viability study of different reverse osmosis membranes for application in the tertiary treatment of wastes from the tanning industry, Desalination 180 (2005) 277–284.
[16] V. Babita, N.P. Shukla, Electrolytic separation of chromium from chrome tannery wastewater, Ind. J. Environ. Health 41 (1999) 43–48.
[17] G. Wójcik, V. Neagu, I. Bunia, Sorption studies of chromium(VI) onto new ion exchanger with tertiary amine, quaternary ammonium and ketone groups, J. Hazard. Mater. 190 (1–3) (2011) 544–552.
[18] A. Senol, Amine extraction of chromium(VI) from aqueous acidic solutions, Sep. Purif. Technol. 36 (2004) 63–75.
[19] S. Hena, Removal of chromium hexavalent ion from aqueous solutions using biopolymer chitosan coated with poly 3-methyl thiophene polymer, J. Hazard. Mater. 181 (2010) 474–479.
[20] K.Z. Elwakeel, Removal of Cr(VI) from alkaline aqueous solutions using chemically modified magnetic chitosan resins, in: Fourteenth International Water Technology Conference, IWTC 14 2010, Cairo, 2010, pp. 133–152.
[21] X. Hua, J. Wang, Y. Liu, X. Li, G. Zenga, Z. Bao, X. Zeng, A. Chen, F. Longa, Adsorption of chromium (VI) by ethylenediamine-modified cross-linked magnetic chitosan resin: isotherms, kinetics and thermodynamics, J. Hazard. Mater. 185 (2011) 306–314.

[22] Y.S. Ho, J.C.Y. Ng, G. McKay, Kinetics of pollutant sorption by biosorbents: review, Sep. Purif. Methods 29 (2) (2000) 189–232.
[23] S. Gupta, B.V. Babu, Removal of toxic metal Cr (VI) from aqueous solutions using sawdust as adsorbent: equilibrium, kinetics and regeneration studies, Chem. Eng. J. 150 (2009) 352–365.
[24] X.S. Wang, Y.P. Tang, S.R. Tao, Kinetics, equilibrium and thermodynamic study on removal of Cr(VI) from aqueous solutions using low-cost adsorbent Alligator weed, Chem. Eng. J. 148 (2009) 217–225.
[25] H.N. Bhatti, A.W. Nasir, M.A. Hanif, Efficacy of *Daucus carota* L. waste biomass for the removal of chromium from aqueous solutions, Desalination 253 (2010) 78–87.
[26] B. Singha, S.K. Das, Biosorption of Cr(VI) ions from aqueous solutions: kinetics, equilibrium, thermodynamics and desorption studies, Colloids Surf. B 84 (2011) 221–232.
[27] S. Chen, Q. Yue, B. Gao, X. Xu, Equilibrium and kinetic adsorption study of the adsorptive removal of Cr(VI) using modified wheat residue, J. Colloid Interface Sci. 349 (2010) 256–264.
[28] O. Ajouyed, C. Hurel, M. Ammari, L. Ben Allal, N. Marmier, Sorption of Cr(VI) onto natural iron and aluminum (oxy)hydroxides: effects of pH, ionic strength and initial concentration, J. Hazard. Mater. 174 (2010) 616–622.
[29] P.K. Pandey, S.K. Sharma, S.S. Sambi, Kinetics and equilibrium study of chromium adsorption on zeolite NaX, Int. J. Environ. Sci. Tech. 7 (2) (2010) 395–404.
[30] R.M. Cheng, S.J. Ou, B. Xiang, Y.J. Li, Q.Q. Liao, Adsorption behavior of hexavalent chromium on synthesized ethylenediamine modified starch, J. Polym. Res. 16 (2009) 703–708.
[31] V. Neagu, Removal of Cr(VI) onto functionalized pyridine copolymer with amide groups, J. Hazard. Mater. 171 (2009) 410–416.
[32] V. Neagu, S. Mikhalovsky, Removal of hexavalent chromium by new quaternized crosslinked poly(4-vinylpyridines), J. Hazard. Mater. 183 (2010) 533–540.
[33] G. Bayramoglu, M.Y. Arica, Synthesis of Cr(VI)-imprinted poly(4-vinyl pyridine-co-hydroxyethyl methacrylate) particles: Its adsorption propensity to Cr(VI), J. Hazard. Mater. 187 (2011) 213–221.
[34] M. Bhaumika, A. Maity, V.V. Srinivasuc, M.S. Onyango, Enhanced removal of Cr(VI) from aqueous solution using polypyrrole/Fe_3O_4 magnetic nanocomposite, J. Hazard. Mater. 190 (1–3) (2011) 381–390.
[35] M.R. Samani, S.M. Borghei, A. Olad, M.J. Chaichi, Removal of chromium from aqueous solution using polyaniline–polyethylene glycol composite, J. Hazard. Mater. 184 (2010) 248–254.
[36] L. Niu, S. Deng, G. Yu, J. Huang, Efficient removal of Cu(II), Pb(II), Cr(VI) and As(V) from aqueous solution using an aminated resin prepared by surface-initiated atom transfer radical polymerization, Chem. Eng. J. 165 (2010) 751–757.
[37] Z. Yong-Gang, S. Hao-Yu, P. Sheng-Dong, H. Mei-Qin, Synthesis, characterization and properties of ethylenediamine-functionalized Fe_3O_4 magnetic polymers for removal of Cr(VI) in wastewater, J. Hazard. Mater. 182 (2010) 295–302.
[38] A. Nastasović, S. Jovanović, D. Đorđević, A. Onjia, D. Jakovljević, T. Novaković, Metal sorption on macroporous poly(GMA-co-EGDMA) modified with ethylene diamine, React. Funct. Polym. 58 (2) (2004) 139–147.
[39] A. Nastasović, D. Jakovljević, Z. Sandić, D. Đorđević, Lj. Malović, S. Kljajević, J. Marković, A. Onjia, Amino-functionalized glycidyl methacrylate based macroporous copolymers as metal ion sorbents, in: M.I. Barroso (Ed.), Reactive and Functional Polymers Research Advances, Nova Science Publishers, New York, 2007, pp. 79–112.
[40] A.A. Atia, A.M. Donia, S.A. Abou-El-Enein, A.M. Yousif, Studies on uptake behaviour of copper(II) and lead(II) by amine chelating resins with different textural properties, Sep. Purif. Technol. 33 (2003) 295–301.
[41] C.Y. Chen, C.L. Chiang, C.R. Chen, Removal of heavy metal ions by a chelating resin containing glycine as chelating groups, Sep. Purif. Technol. 54 (2007) 396–403.
[42] C. Liu, R. Bai, L. Hong, T. Liu, Functionalization of adsorbent with different aliphatic polyamines for heavy metal ion removal: characteristics and performance, J. Colloid Interface Sci. 345 (2010) 454–460.
[43] Z.P. Sandić, A.B. Nastasović, N.P. Jović-Jovičić, A.D. Milutinović-Nikolić, D.M. Jovanović, Sorption of textile dye from aqueous solution by macroporous amino-functionalized copolymer, J. Appl. Polym. Sci. 121 (1) (2011) 234–242.
[44] B.F. Senkal, F. Bildik, E. Yavuz, A. Sarac, Preparation of poly(glycidyl methacrylate) grafted sulfonamide based polystyrene resin with tertiary amine for the removal of dye from water, React. Funct. Polym. 67 (12) (2007) 1471–1477.
[45] K.Z. Elwakeel, M. Rekaby, Efficient removal of reactive black 5 from aqueous media using glycidyl methacrylate resin modified with tetraethelenepentamine, J. Hazard. Mater. 188 (1–3) (2011) 10–18.
[46] A. Nastasović, Z. Sandić, Lj. Suručić, D. Maksin, D. Jakovljević, A. Onjia, Kinetics of hexavalent chromium sorption on amino-functionalized macroporous glycidyl methacrylate copolymer, J. Hazard. Mater. 171 (1–3) (2009) 153–159.
[47] R.V. Hercigonja, D.D. Maksin, A.B. Nastasović, S.S. Trifunović, P.B. Glodić, A.E. Onjia, Adsorptive removal of technetium-99 using macroporous poly(GMA-co-EGDMA) modified with diethylene t5riamine, J. Appl. Polym. Sci. (2011), doi:10.1002/app.34693.
[48] D.C. Sharma, C.F. Forster, The treatment of chromium wastewaters using the sorptive potential of leaf mould, Bioresour. Technol. 49 (1) (1994) 31–40.
[49] P.A. Webb, C. Orr, Analytical Methods in Fine Particle Technology, Micromeritics Instrument Corporation, Norcross, 1997.
[50] A.B. Nastasović, Z.P. Sandić, D.D. Maksin, A.E. Onjia, A.D. Milutinović-Nikolić, D.M. Jovanović, Macroporous and non-porous amino-functionalized glycidyl methacrylate based copolymers for hexavalent chromium sorption, in: M.P. Salden (Ed.), Chromium: Environmental, Medical and Materials Studies, Nova Science Publishers, New York, 2011, in press.
[51] G. Yang, S.Y. Fu, J.P. Yang, Preparation and mechanical properties of modified epoxy resins with flexible diamines, Polymer 48 (2007) 302–310.
[52] S.J. Park, Y.S. Jang, Pore structure and surface properties of chemically modified activated carbons for adsorption mechanism and rate of Cr(VI), J. Colloid Interface Sci. 249 (2002) 458–463.
[53] T. Karthikeyan, S. Rajgopal, L.R. Miranda, Chromium (VI) adsorption from aqueous solution by Hevea Brasilinesis sawdust activated carbon, J. Hazard. Mater. B124 (2005) 192–199.
[54] International Atomic Energy Agency (IAEA), Application of ion exchange processes for the treatment of radioactive waste and management of spent ion exchangers, technical reports series No. 408. IAEA, Vienna; 2002.
[55] Y.S. Ho, Review of second-order models for adsorption systems, J. Hazard. Mater. B136 (2006) 681–689.
[56] S. Lagergren, About the theory of so-called adsorption of soluble substances, K. Sven. Vetenskapsakad. Handl. 24 (4) (1898) 1–39.
[57] D.L. Sparks, Kinetics of Soil Chemical Processes, Academic Press Inc., New York, 1989.
[58] W.J. Weber, J.C. Morris, Kinetics of adsorption on carbon from solution, J. Sanit. Eng. Div., Am. Soc. Civ. Eng. 89 (1963) 31–60.
[59] G.E. Boyd, A.M. Adamson, L.S. Myers, The exchange adsorption of ions from aqueous solution by organic zeolites II. Kinetics, J. Am. Chem. Soc. 69 (1947) 2836–2842.
[60] E. Tutem, R. Apak, C.F. Unal, Adsorptive removal of chlorophenols from water by bituminous shale, Water Res. 32 (8) (1998) 2315–2324.
[61] W. Plazinski, W. Rudzinski, A. Plazinska, Theoretical models of sorption kinetics including a surface reaction mechanism: a review, Adv. Colloid Interface Sci. 152 (2009) 2–13.
[62] H. Zhang, Y. Tang, D. Cai, X. Liu, X. Wang, Q. Huang, Z. Yu, Hexavalent chromium removal from aqueous solution by algal bloom residue derived activated carbon: equilibrium and kinetic studies, J. Hazard. Mater. 181 (2010) 801–808.
[63] A.S. Özcan, A. Özcan, Adsorption of acid dyes from aqueous solutions onto acid-activated bentonite, J. Colloid Interface Sci. 276 (2004) 39–46.
[64] A.M. Donia, A.A. Atia, W.A. Al-amrani, A.M. El-Nahas, Effect of structural properties of acid dyes on their adsorption behaviour fromaqueous solutions by amine modified silica, J. Hazard. Mater. 161 (2009) 1544–1550.
[65] Y.S. Ho, J.F. Porter, G. McKay, Equilibrium isotherm studies for the sorption of divalent metal ions onto peat: copper, nickel and lead single component systems, Water Air Soil Pollut. 141 (2002) 1–33.
[66] I.J. Langmuir, The adsorption of gases on plane surfaces of glass, mica and platinum, J. Am. Chem. Soc. 40 (1918) 1361–1403.
[67] H.M.F. Freundlich, Over the adsorption in solution, J. Phys. Chem. 57 (1906) 385–470.
[68] M.J. Tempkin, V. Pyzhev, Kinetics of ammonia synthesis on promoted iron catalysts, Acta Physicochim. URSS 12 (1940) 217–222.
[69] D. Mohan, C.U. Pittman, Activated carbons and low cost adsorbents for remediation of tri- and hexavalent chromium from water, J. Hazard. Mater. B137 (2006) 762–811.
[70] E. Alemayehu, S. Thiele-Bruhn, B. Lennartz, Adsorption behaviour of Cr(VI) onto macro and micro-vesicular volcanic rocks from water, Sep. Purif. Technol. 78 (2011) 55–61.
[71] S.S. Liu, Y.Z. Chen, L.D. Zhang, G.M. Hua, W. Xu, N. Li, Y. Zhang, Enhanced removal of trace Cr(VI) ions from aqueous solution by titanium oxide–Ag composite adsorbents, J. Hazard. Mater. 190 (1–3) (2011) 723–728.
[72] V. Marjanović, S. Lazarević, I. Janković-Častvan, B. Potkonjak, Đ. Janaćković, R. Petrović, Chromium (VI) removal from aqueous solutions using mercaptosilane functionalized sepiolites, Chem. Eng. J. 166 (2011) 198–206.
[73] Y. Zeng, H. Woo, G. Lee, J. Park, Removal of chromate from water using surfactant modified Pohang clinoptilolite and Haruna chabazite, Desalination 257 (2010) 102–109.
[74] X.S. Wang, Z.Z. Li, Removal of Cr(VI) from aqueous solution by newspapers, Desalination 249 (2009) 175–181.
[75] J. Anandkumara, B. Mandalb, Adsorption of chromium(VI) and Rhodamine B by surface modified tannery waste: kinetic, mechanistic and thermodynamic studies, J. Hazard. Mater. 186 (2011) 1088–1096.
[76] X.F. Suna, C. Liub, Y. Maa, S.G. Wanga, B.Y. Gaoa, X.M. Li, Enhanced Cu(II) and Cr(VI) biosorption capacity on poly(ethylenimine) grafted aerobic granular sludge, Colloids Surf. B 82 (2011) 456–462.
[77] D. Mohan, S. Rajputa, V.K. Singh, P.H. Steele, C.U. Pittman Jr., Modeling and evaluation of chromium remediation from water using low cost bio-char, a green adsorbent, J. Hazard. Mater. 188 (2011) 319–333.
[78] A.B. Albadarin, A.H. Al-Muhtaseb, G.M. Walker, S.J. Allen, M.N.M. Ahmad, Retention of toxic chromium from aqueous phase by H3PO4-activated lignin: effect of salts and desorption studies, Desalination 274 (2011) 64–73.
[79] W. Liu, J. Zhang, C. Zhang, Y. Wang, Y. Li, Adsorptive removal of Cr(VI) by Fe-modified activated carbon prepared from Trapa natans husk, Chem. Eng. J. 162 (2010) 677–684.

[80] E. Oguz, B. Keskinler, Determination of adsorption capacity and thermodynamic parameters of the PAC used for bomaplex red CR-L dye removal, Colloids Surf., A 268 (2005) 124–130.
[81] R.S. Juang, F.C. Wu, R.L. Tseng, The ability of activated clay for the adsorption of dyes from aqueous solutions, Environ. Technol. 18 (5) (1997) 525–531.
[82] S. Glasston, K.J. Laidler, H. Eyring, The Theory of Rate Processes, McGraw-Hill, New York, 1941.
[83] V.K. Gupta, D. Mohan, S. Sharma, Removal of lead from wastewater using bagasse fly ash—a sugar industry waste material, Sep. Sci. Technol. 33 (1998) 1331–1343.
[84] E. Malmoc, Y. Nuhoglu, Determination of kinetic and equilibrium parameters of the batch adsorption of Cr(VI) onto waste acorn of Quercus ithaburensis, Chem. Eng. Process. 46 (2007) 1020–1029.